Plant Cell Physiol. 43(10): 1154–1164 (2002)

Detection of Singlet Oxygen and Superoxide with Fluorescent Sensors in Leaves Under Stress by Photoinhibition or UV Radiation

Éva Hideg [1, 4], Csengele Barta [1], Tamás Kálai [2], Imre Vass [1], Kálmán Hideg [2] and Kozi Asada [3]

[1] *Institute of Plant Biology, Biological Research Center, H-6701 Szeged, P.O. Box 521, Hungary*
[2] *Department of Organic and Medicinal Chemistry, University of Pécs, H-7643 Pécs, P.O. Box 99, Hungary*
[3] *Department of Biotechnology, Faculty of Engineering, Fukuyama University, Gakuen-cho 1, Fukuyama, 729-0292 Japan*

In order to understand the physiological functions of reactive oxygen species (ROS) generated in leaves, their direct measurement in vivo is of special importance. Here we report experiments with two dansyl-based ROS sensors, the singlet oxygen specific DanePy and HO-1889NH, which is reactive to both singlet oxygen and superoxide radicals. Here we report in vivo detection of $^1O_2$ and $O_2^{-\bullet}$ by fluorescence quenching of two dansyl-based ROS sensors, the $^1O_2$ specific DanePy and HO-1889NH, which was reactive with both $^1O_2$ and $O_2^{-\bullet}$. The ROS sensors were administered to spinach leaves through a pinhole, and then the leaves were exposed to either excess photosynthetically active radiation or UV (280–360 nm) radiation. Microlocalization of the sensors' fluorescence and its ROS-induced quenching was followed with confocal laser scanning microscopy and with fluorescence imaging. These sensors were specifically localized in chloroplasts. Quenching analysis indicated that the leaves exposed to strong light produced $^1O_2$, but hardly any $O_2^{-\bullet}$. On the other hand, the dominant ROS in UV-irradiated leaves was $O_2^{-\bullet}$, while $^1O_2$ was minor.

Keywords: Reactive oxygen — Double (fluorescent and spin) sensor — Photoinhibition — Ultraviolet light.

Abbreviations: DanePy, 3-[*N*-(β-diethylaminoethyl)-*N*-dansyl] aminomethyl-2,2,5,5-tetramethyl-2,5-dihydro-1*H*-pyrrole; HO-1889NH, 3-(*N*-dansyl)aminomethyl-2,2,5,5-tetramethyl-2,5-dihydro-1*H*-pyrrole; LSM, laser scanning microscopy; ROS, reactive oxygen species; PAR, photosynthetically active radiation; PS, photosystem; UV-A, 320–360 nm ultraviolet radiation; UV-B, 280–320 nm ultraviolet radiation.

Part of these results was reported in a preliminary form at the 12th International Congress on Photosynthesis, 18-23 August 2001, Brisbane (Australia).

Introduction

Plants rely on light as essential energy source and signal for photosynthesis, biosynthesis of cell components, photomorphogenesis and development. Light requirements are largely variable in terms of intensities and spectral distribution, depending on the plant species, developmental stage, and are also affected by acclimation to local environmental conditions. For photosynthesis, photosynthetically active radiation (PAR) from sunlight is essential. This shows large seasonal and diurnal changes, and its intensity is also influenced by meteorological factors. When the photon intensity is within the range of the utilizing capacity of chloroplasts for CO_2-fixation, the generation rate of reactive oxygen species (ROS) is very low, and these molecules are effectively scavenged. However, when either PAR intensity is higher or the utilizing capacity is lowered by environmental stresses, excess photons promote the production of ROS and cause the photoinhibition (PI) of photosynthesis. Under such conditions, PSII is preferentially damaged (for reviews see Powles 1984, Barber and Andersson 1992).

In addition to excess PAR, UV-B (280–320 nm) radiation from sunlight also inhibits photosynthesis (for reviews see Teramura and Sullivan 1994, Vass 1997). Similarly to the photoinhibition by excess PAR, UV also results in the inactivation of PSII electron transport (Bornman 1989) and damage to a PSII core protein, D1 (Renger et al. 1989, Vass et al. 1996). However, there are differences in the effect of the two light stresses. For instance, the primary site of their electron transport inactivation in PSII (Kulandaivelu and Noorudeen 1983), the cleavage site of D1 (Greenberg et al. 1989), whether they cleave PSII core proteins other than D1 (Renger et al. 1989), and the oxygen dependence of their effect in vitro (Aro et al. 1993, Friso et al. 1994).

Under physiological or mild stress conditions, the steady state ROS concentration is kept low by the scavenging activity of enzymes and other antioxidants (for reviews see Asada 1994, Asada 1999). Also, active de novo synthesis of D1 protein (reviewed by Aro et al. 1993) recovers PSII functions rapidly. Artificial strong stress as well as a combination of several stress factors in the field may result in conditions when the antioxidant system and repair mechanisms are not able to prevent or counterbalance oxidative damage. ROS appear to be key molecules under many biotic and abiotic stress conditions and are considered in a variety of roles, such as oxidants of target molecules, primary elicitors of damage, propagators, and signal molecules for the activation of defense or repair. With the exception of H_2O_2, the half-lives of ROS are very short in water: several s for superoxide anion radicals ($O_2^{-\bullet}$) and microseconds for singlet oxygen ($^1O_2$), and thus their diffusion distances from the generation sites are very short (Halliwell and

[4] Corresponding author: E-mail, ehideg@nucleus.szbk.u-szeged.hu; Fax: +36-62-433-434.

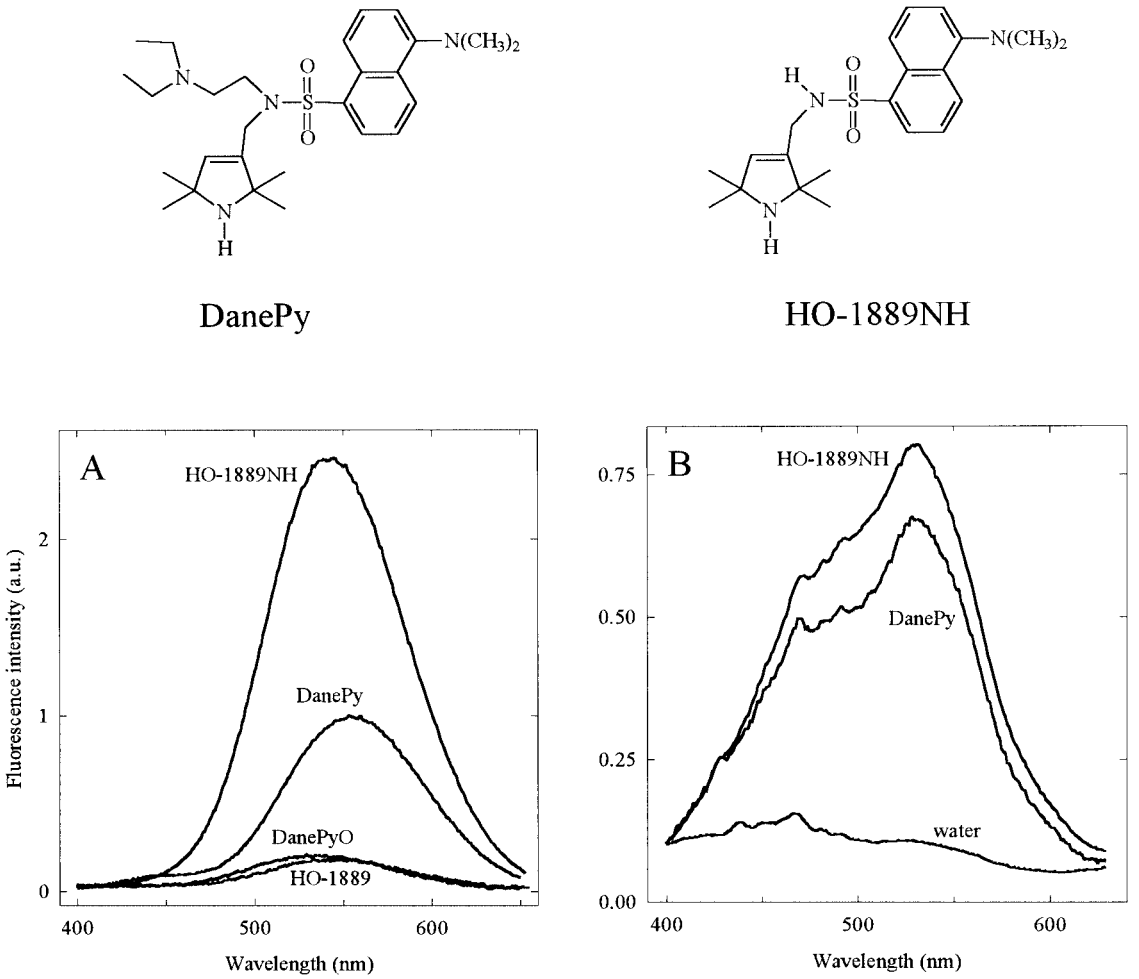

Fig. 1 Structures and 330 nm excited fluorescence spectra of the dansyl-based ROS sensors applied in this study. (A) Fluorescence spectra of 0.2 mM DanePy and 0.2 mM HO-1889NH, and their corresponding nitroxide adducts DanePyO and HO-1889 at 0.2 mM in 50 mM Na-phosphate, pH 7.2, containing 5% ethanol. (B) Fluorescence spectra of spinach leaf infiltrated through a pinhole with 1 mM DanePy or 1 mM HO-1889NH, and the blue-green intrinsic fluorescence of a leaf infiltrated with water only. All fluorescence spectra are normalised to the peak intensity of 0.2 mM DanePy in (A).

Gutteridge 1999). Therefore, for effective in vivo detection of ROS, specific sensors and probes should be localized at a site where ROS is photoproduced.

Spin trapping EPR spectroscopy proved useful in detecting ROS in isolated photosynthetic membranes exposed to strong light (Hideg et al. 1994a, Hideg et al. 1995, Hirayama et al. 1995, Yruela et al. 1996), or UV radiation (Hideg and Vass 1996). However, its application to intact leaves was limited due to the reduction of spin adducts to the hydroxylamine form by leaf metabolites (Hideg et al. 1994b) and to technical problems caused by the high water content of leaves (Hideg et al. 2000a). Double (spin and fluorescent) ROS sensors, consisting of a fluorophore and a nitroxide precursor were found more stable in leaves than spin traps. In the absence of ROS, the double sensors are highly fluorescent but EPR silent. Upon reacting with ROS, conversion of the spin trap moiety into an EPR active nitroxide results in partial fluorescence quenching (Green et al. 1990). This principle was realised in a dansyl-based $^1O_2$ sensor, DanePy (Kálai et al. 1998, Hideg et al. 2000a). Using DanePy, we have shown the generation of $^1O_2$ in leaves by strong PAR (under photoinhibitory conditions) but not by UV-B radiation (Hideg et al. 1998, Hideg et al. 2000b). For these studies, the ROS sensor was vacuum infiltrated into leaf discs. However, vacuum infiltration of the sensor may destroy cell structures and induce the destabilization of the sensor by leaf metabolites. Further, it enhances the non-specific blue-green fluorescence when excited by UV (Chapelle et al. 1984), which disturbs the measurement of DanePy fluorescence quenching to follow $^1O_2$ generation.

In the present study, we compared methods to administer ROS sensors into leaves in order to minimize the above interferences and found that the infiltration through a pinhole gave

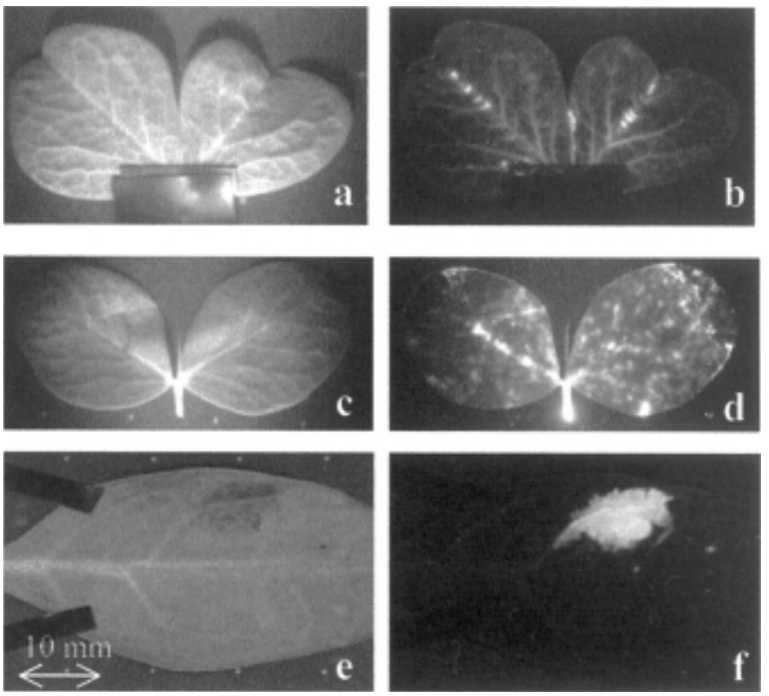

Fig. 2 Images of garden pea (a–d) and tobacco (e–f) leaves infiltrated with 2 mM DanePy using osmotic uptake — transpiration stream — through the petiole (a, b), vacuum infiltration (c, d) or syringe infiltration through a pinhole (e–f). (a, c, e) are photographic images, (b, d, f) are images of 410–640 nm fluorescence excited with UV (310 nm) light.

few artefacts. Using this method, we conducted a comparative study of ROS production in spinach leaves exposed to either photoinhibition by excess PAR or UV radiation, using the $^1O_2$ sensor DanePy and a new dansyl-based sensor, HO-1889NH, which is capable of detecting $^1O_2$ and $O_2^{-\bullet}$. Stress-induced quenching of the ROS sensors' fluorescence was followed in leaf tissue by confocal laser scanning microscopy (LSM), as well as by fluorescence imaging.

Results

Fluorescence and specificity of ROS sensors

Fig. 1 shows the structures and 330 nm excited fluorescence emission spectra of the two dansyl-based double sensors used in this study. Fluorescence emission from the corresponding nitroxides, DanePyO and HO-1889, were 5–6 times lower than that of the ROS sensors, DanePy and HO-1889NH (Fig. 1A), respectively. When infiltrated into spinach leaves, fluorescence of the ROS sensors was less intense, due to absorption of both the excitation light and the emitted ROS sensor fluorescence in leaf tissue (Fig. 1B). Fluorescence emission spectra of the sensors were superimposed on the UV-excited blue-green autofluorescence of green leaves (Chapelle et al. 1984) (Fig. 1B). The autofluorescence from spinach leaves was relatively lower than from other plants, for example cereals (data not shown). Thus, with adequate infiltration through a pinhole (detailed below), the intrinsic fluorescence in the 515–550 nm spectral region was less than 10% of the sensors' fluorescence.

Specificities of DanePy and HO-1889NH for ROS were characterized by quenching of their fluorescence in response to chemically generated ROS (Table 1). Although the structures of DanePy and HO-1889NH are very similar to each other — different only in a side chain — they showed different specificities. DanePy was specific to $^1O_2$ as shown previously (Kálai et al. 1998). HO-1889NH showed lower sensitivity to $^1O_2$, but had an additional reactivity to $O_2^{-\bullet}$. Fluorescence of the two sensors was not quenched by either hydroxyl radicals ($^{\bullet}OH$) or H_2O_2 (Table 1). It is also worth noting that the fluorescence of the tested ROS sensors was not influenced by the presence of iron ions — neither in the Fe(II) (ammonium ferrous sulfate), nor in the Fe(III) ($FeCl_3$) form (Hankovszky et al. 2001).

Infiltration methods of ROS sensors and their effect on photosynthesis

Distribution of the ROS sensor in leaves was largely

Table 1 Relative changes in the fluorescence emission of the ROS sensors upon reacting with various ROS from chemical sources

	No addition	$^1O_2$	H_2O_2	$^{\bullet}OH$	$O_2^{-\bullet}$
DanePy	100%	35%	97%	98%	93%
HO-1889NH	100%	60%	98%	96%	65%

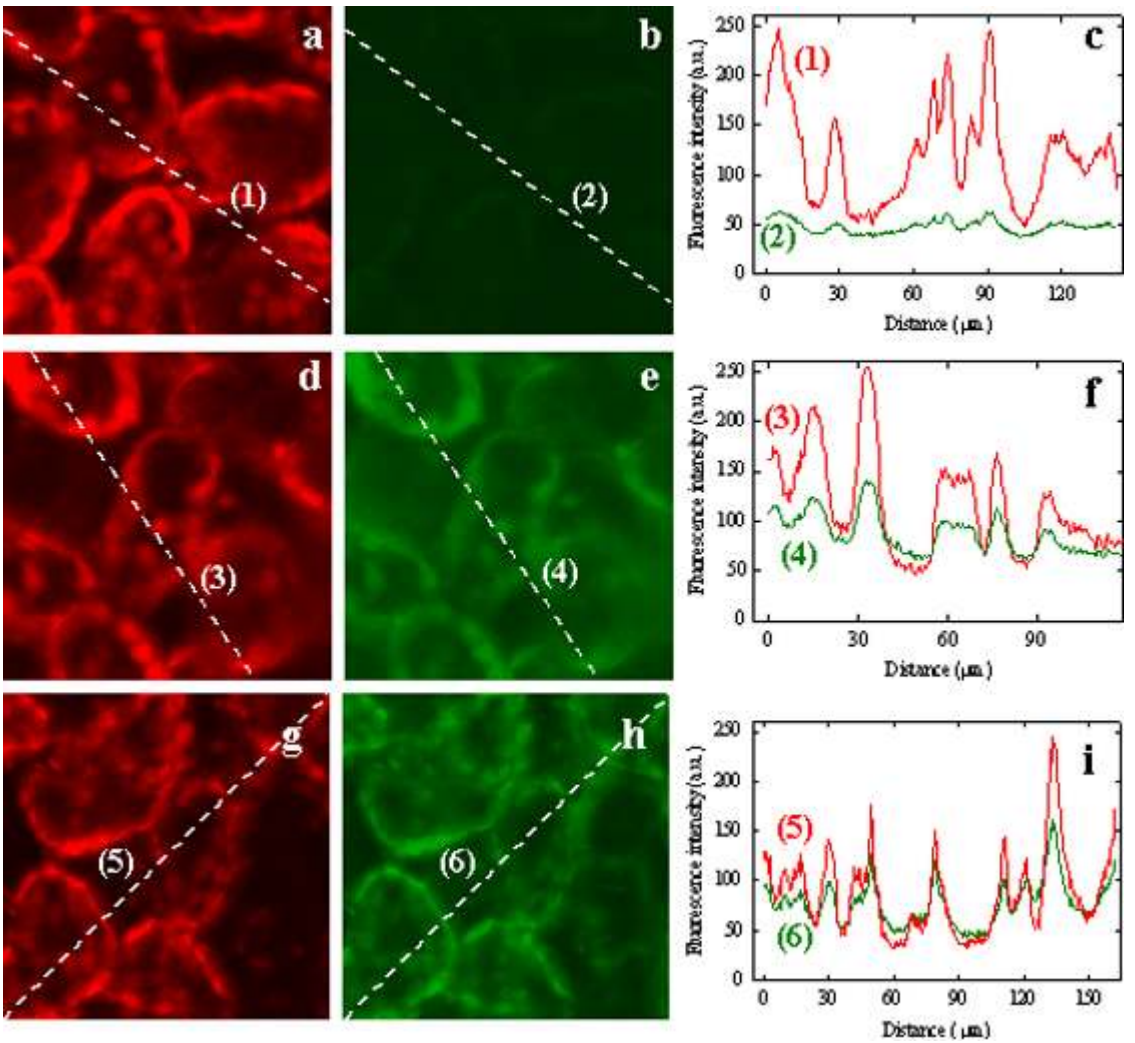

Fig. 3 LSM images of 351 nm excited red (λ >650 nm) (a, d, g) and green (515< λ <550 nm) (b, e, h) fluorescence detected in spinach leaves infiltrated with either 5% aqueous ethanol (a, b), 1 mM DanePy (d, e) or 1 mM HO-1889NH (g, h) in water containing 5% ethanol. Image size 115×115 μm. Graphs (c, f, i) compare intensities of red and green fluorescence along the numbered, right to left diagonal lines shown in the images.

affected by the infiltration method. Neither uptake through the transpiration system from the petiole, nor vacuum infiltration in a plastic syringe provided uniform distribution of the sensor in leaf tissues. The transpiration uptake through the leaf petiole was poor, and sensor fluorescence was mainly observed in the vascular tissue (Fig. 2b). In vacuum-infiltrated leaves, DanePy was deposited in the petiole and was not continually distributed in the leaf tissue (Fig. 2d). On the other hand, infiltration through a pinhole resulted in uniform distribution of the sensor in mesophyll cells (Fig. 2f). Typical diameter of the infiltrated area was 8–12 mm diameter, depending on the proximity of vascular tissue. Distribution of HO-1889NH was the same as that of DanePy (data not shown).

Effects of the vacuum infiltration and the infiltration through a pinhole were compared for spinach leaves with and without DanePy. PSII activity, as measured by variable chlorophyll fluorescence (F_v/F_m = 0.78 in untreated leaves), was not affected by the infiltration through a pinhole, but decreased by about 10% by vacuum infiltration. CO_2 assimilation rate (6.0 CO_2 μmol m^{-2} s^{-1}) was inactivated by about 70% by the vacuum infiltration, but only by 20% by the infiltration through a pinhole (Table 2). The presence of DanePy in the infiltrating solution showed little effect, indicating that activity loss was mainly due to structural damage to leaf cells and chloroplasts during the infiltration process rather than to DanePy. Further, vacuum infiltration enhanced the UV-excited blue-green intrinsic leaf fluorescence (data not shown), probably due to structural damage of leaf tissue, and thus disturbed the ROS sensor fluorescence quenching analysis. Such disturbance was, however, much lower when the sensors were applied by infiltration

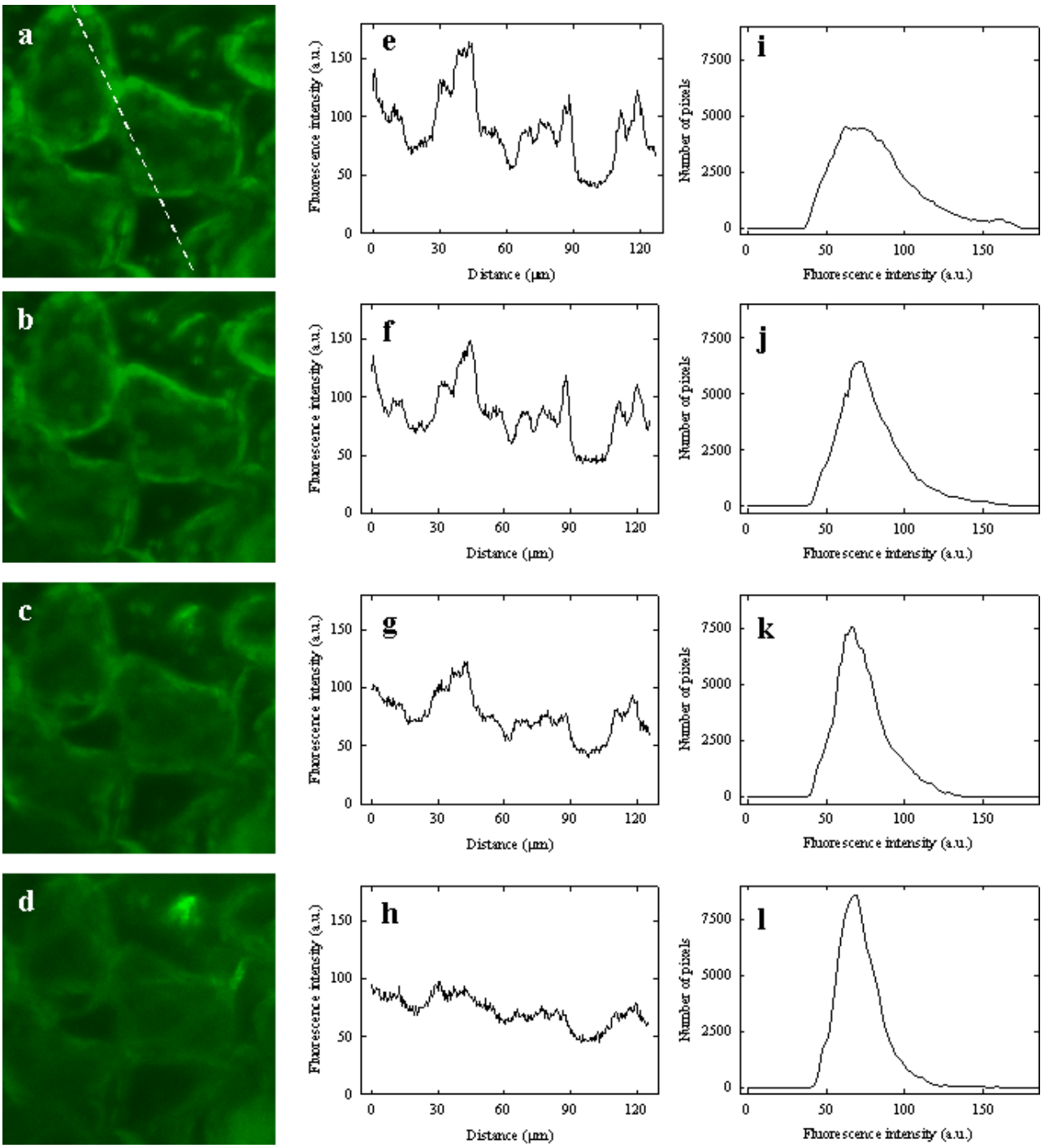

Fig. 4 LSM images of 351 nm excited green (515< λ <550 nm) fluorescence from a DanePy infiltrated spinach leaf (a–d), fluorescence intensity along the diagonal line showed in (a) (e–h) and histograms of fluorescence images (i–l). After infiltration, the leaf was exposed to 1,800 μmol m^{-2} s^{-1} PAR for 0 min (a, e, i), 15 min (b, f, j), 30 min (c, g, k) and 45 min (d, h, l). LSM image size: 115×115 μm.

through a pinhole (Fig. 1B). Therefore, in the following experiments, the ROS sensors were infiltrated to leaf tissue by the pinhole method.

ROS sensors are localized in chloroplasts as detected by confocal LSM

Fig. 3 illustrates typical microscopic distribution of DanePy and HO-1889NH in spinach leaves. The ROS sensors

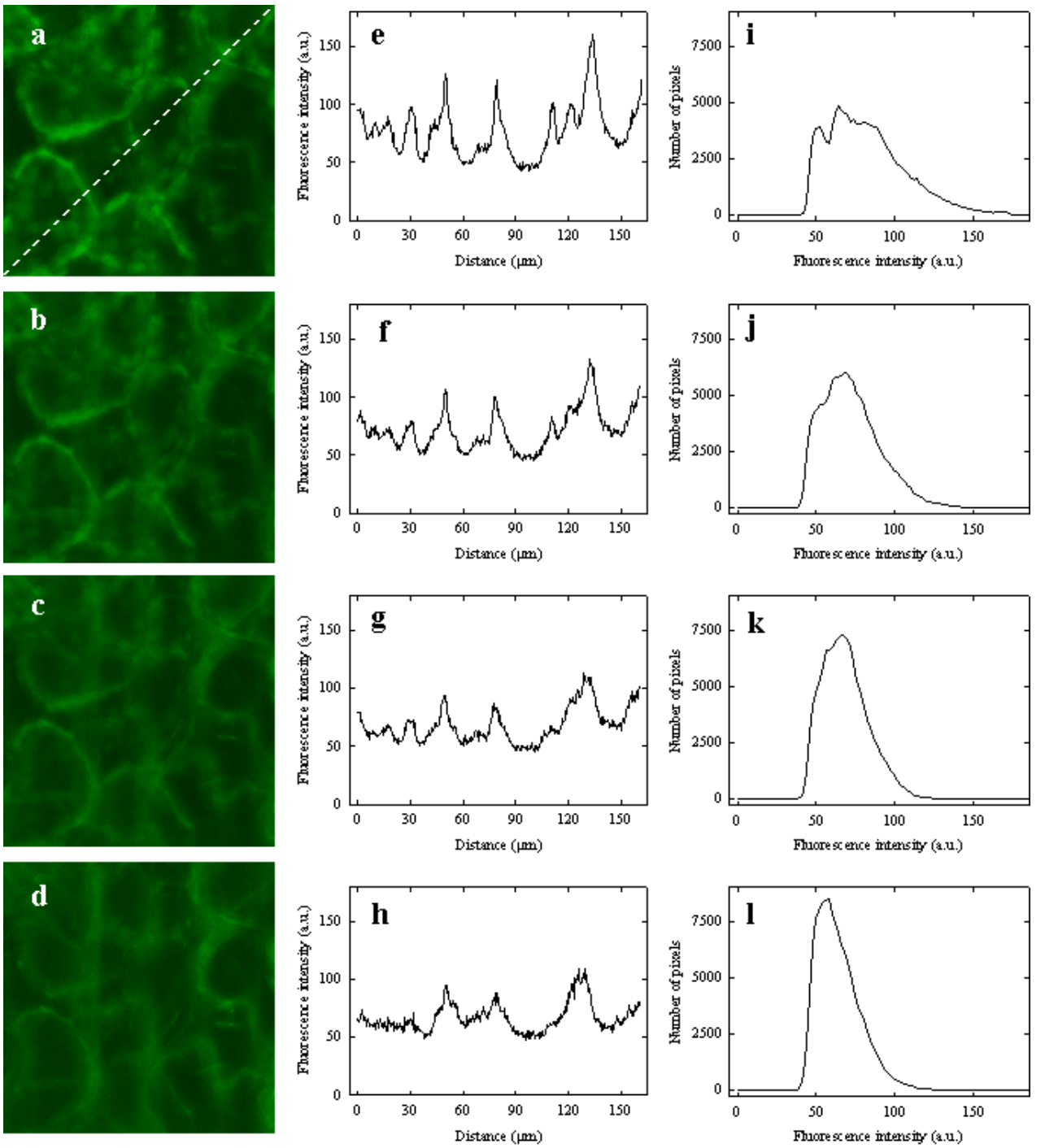

Fig. 5 LSM images of 351 nm excited green (515< λ <550 nm) fluorescence from a HO-1889NH infiltrated spinach leaf (a–d), fluorescence intensity along the diagonal line showed in (a) (e–h) and histograms of fluorescence images (i–l). After infiltration, the leaf was exposed to photoinhibition for 0 min (a, e, i), 15 min (b, f, j), 30 min (c, g, k) and 45 min (d, h, l). LSM image size: 115×115 μm.

were infiltrated through pinholes and their cellular localisation was detected by their UV-induced green (515–550 nm) fluorescence by confocal LSM. UV-induced red chlorophyll fluorescence identified chloroplasts, which were localized mainly along the plasma membrane of the cells (Fig. 3a, d, g). The UV-inducible green intrinsic fluorescence was low in leaves infiltrated with 5% aqueous ethanol without the ROS sensor (Fig. 3b), and its location did not coincide with the red chloro-

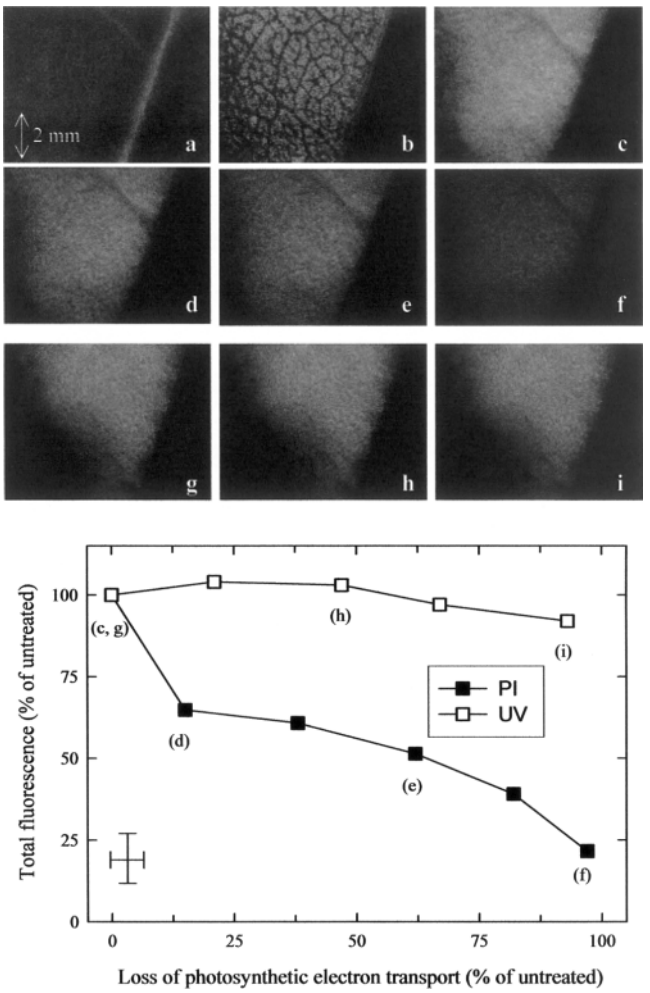

Fig. 6 Images of DanePy infiltrated spinach leaves acquired by a microscope and digital image analysing system (see Materials and Methods). Leaf pictures in reflected (a) and transmitted (b) visible illumination. UV (295–375 nm) excited images of 410–640 nm fluorescence from the same leaf segment as in (a) and (b) after 0 min (c), 15 min (d), 45 min (e) and 75 min (f) exposure to 1,800 μmol m^{-2} s^{-1} PAR and from another leaf after irradiation with broad band UV (280–360 nm) for 0 min (g), 30 min (h) and 60 min (i). The graph below the images compares the stress-induced loss in total DanePy fluorescence in leaves photoinhibited by excess PAR (full squares) and in UV irradiated (empty squares) leaves as a function of photosynthetic electron transport loss. Data points which were calculated from images in the upper part of the figure are marked with corresponding letters. Typical errors in total fluorescence and in loss of photosynthetic yield parameter were calculated from three independent experiments and are shown as vertical and horizontal error bars, respectively, in the lower left corner of the figure.

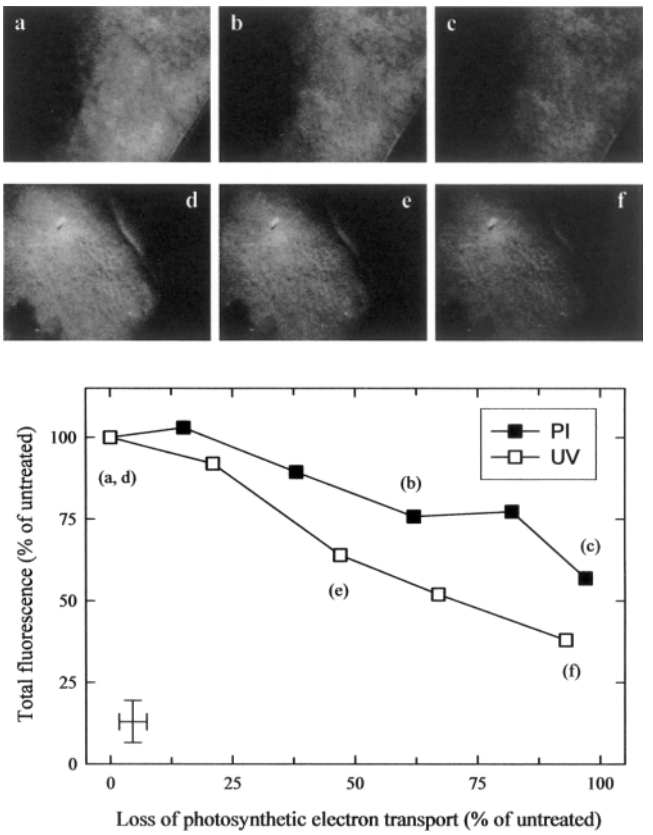

Fig. 7 UV (295–375 nm) excited images of 410–640 nm fluorescence in HO-1889NH infiltrated spinach leaves. After infiltration, one leaf segment was exposed to photoinhibition by 1,800 μmol m^{-2} s^{-1} PAR for 0 min (a), 45 min (b) and 75 min (c) and another leaf was irradiated broad band UV (280–360 nm) for 0 min (d), 30 min (e) and 60 min (f). The graph below the images compares the stress-induced loss in total HO-1889NH fluorescence in photoinhibited (full squares) and in UV irradiated (empty squares) leaves as a function of photosynthetic electron transport loss. Data points which were calculated from images in the upper part of the figure are marked with corresponding letters. Typical errors in total fluorescence and in loss of photosynthetic yield parameter were calculated from three independent experiments and are shown as vertical and horizontal error bars, respectively, in the lower left corner of the figure.

phyll fluorescence (Fig. 3c). In this way, the green fluorescence from DanePy and HO-1889NH infiltrated leaves (Fig. 3e and h, respectively) was emitted almost entirely from the ROS sensors. Comparison of the intensity distribution of green fluorescence from the ROS sensors with that of red chlorophyll fluorescence showed that both DanePy and HO-1889NH penetrated into chloroplasts (Fig. 3f and i, respectively). Intensity profiles of the green fluorescence at the local minima between these peaks was always above zero, which represent the emission from the ROS sensors in the symplastic or apoplastic compartment and the intrinsic autofluorescence (Fig. 3e, h). However, ratios of ROS fluorescence from chloroplastic and symplastic origin do not necessarily reflect quantitative distribution, as the fluorescence yield of the sensors may depend on their environment (for example, aqueous or membrane).

Fluorescence from the ROS sensors in chloroplasts was quenched when the infiltrated leaves were exposed to excess PAR. Fig. 4 and 5 document changes in the intensities of

Table 2 Comparison of variable chlorophyll fluorescence (F_v/F_m) and CO_2 assimilation rate in untreated and DanePy or water infiltrated spinach leaves

Treatment	F_v/F_m	CO_2 assimilation rate (μmol m^{-2} s^{-1})
Untreated	0.78±0.08	6.0±0.41
Vacuum infiltrated with DanePy	0.70±0.07	0.8±0.35
Vacuum infiltrated with 5% ethanol	0.73±0.03	2.3±0.45
Pinhole infiltrated with DanePy	0.78±0.05	5.1±0.29
Pinhole infiltrated with 5% ethanol	0.77±0.07	4.9±0.49

DanePy was infiltrated in 1 mM water solution (containing 5% ethanol) either by vacuum infiltration or through a pinhole (see Materials and Methods for details). For reference, leaves were also treated with the infiltrating solution only, i.e. without DanePy.

DanePy and HO-1889NH fluorescence, respectively, inside the mesophyll cells during exposures for up to 45 min. For quantitative analysis, fluorescence intensity profiles (Fig. 4e–h, e–h) were plotted along diagonal lines in the LSM pictures (Fig. 4a, 5a). For both ROS sensors, fluorescence intensities decreased, especially in chloroplasts, with increasing exposure times (Fig. 4e–h, 5e–h). The sharp peaks in DanePy fluorescence intensity profiles observed in untreated samples (Fig. 4e) almost completely disappeared (Fig. 4h) and those of HO-1889NH fluorescence decreased by at least 50% (Fig. 5e, h). The green fluorescence of either sensors was only affected by excess PAR in compartments other than chloroplasts. Excess PAR induced decline of ROS fluorescence is also illustrated using histograms calculated from all data points in the LSM images. Shifting of histogram maxima to the left, towards lower fluorescence intensities and the conversion of broad peaks into sharper ones were observed with increasing exposure times to excess PAR for both DanePy (Fig. 4i–l) and HO-1889NH (Fig. 5i–l).

Quenching of ROS sensor fluorescence by exposing leaves to excess PAR or UV

Data in Fig. 4 clearly indicated, that $^1O_2$ was generated by excess PAR, mostly in chloroplasts. In confocal LSM experiments, excess PAR was applied to leaf cuttings. In order to estimate ROS production in whole leaves quantitatively, the ROS sensors were infiltrated to spinach leaves through pinholes. A photographic image of a leaf area infiltrated with DanePy is shown in Fig. 6a. Usually, the pinhole itself was not visible and the infiltrated area was obvious in pictures taken with transillumination only, due to its higher water content as compared to non-infiltrated tissue (Fig. 6b). Infiltrated leaves were allowed to dry for 10 min, then a UV-induced 410–640 nm fluorescence image of the area was taken (Fig. 6c). Under these experimental conditions, the UV-excited blue-green intrinsic fluorescence of the leaf was negligible, since fluorescence was detected from the infiltrated area only (compare Fig. 6b, c). The fluorescence of both ROS sensors was stable in the dark (data not shown) but quenched by exposing the leaves to excess PAR (Fig. 6, 7).

Fluorescence images in Fig. 6 show the effects of excess PAR and UV radiation on the fluorescence of DanePy infiltrated leaves (Fig. 6c–f, g–i, respectively). The leaf was exposed to excess PAR for 75 min, which resulted in gradual quenching of the sensor's fluorescence (Fig. 6c–f). On the other hand, exposure to UV-A and UV-B radiation (280–360 nm) for 60 min affected DanePy fluorescence to a small extent only, although PSII electron transport rate was inactivated to less than 10% (Fig. 6g–i). In the graph below the images, there is a quantitative analysis of these and other, similar, sets of experiments. Quantitative analysis confirmed conclusions from visual information of the images, and showed that the exposure of spinach leaves to excess PAR resulted in progressive loss of DanePy fluorescence. On the other hand, UV radiation had little effect on fluorescence from the $^1O_2$ sensor (Fig. 6).

The $^1O_2$ and $O_2^{-\bullet}$ reactive HO-1889NH was infiltrated into the leaves and its fluorescence was followed during exposure to the same excess PAR and UV treatments as in Fig. 6. Images in Fig. 7a–c show that, similarly to DanePy, HO-1889NH fluorescence was also quenched during exposing the leaf to excess PAR. As at the bottom of Fig. 7, where data from Fig. 7a–c are combined with values from other sets of the same experiment, quenching of HO-1889NH fluorescence was about 50% smaller than that of DanePy under similar conditions (Fig. 6). While UV radiation did not cause significant quenching in DanePy fluorescence (Fig. 6g–i), the same treatment of HO-1889NH infiltrated leaves caused strong, progressive quenching in the fluorescence of this ROS sensor, to a larger extent than excess PAR (Fig. 7d–e). These observations indicated that excess PAR caused $^1O_2$ generation but practically no $O_2^{-\bullet}$, while $O_2^{-\bullet}$ gave rise to most quenching of HO-1889NH fluorescence in UV-exposed leaves.

Discussion

Both the $^1O_2$ sensitive DanePy and the $^1O_2$ and $O_2^{-\bullet}$ reactive HO-1889NH (Table 1) are capable of quenching more than 80% of their fluorescence upon reacting with their target ROS (Fig. 1A). Local infiltration of a leaf segment through a pin-

hole proved a mild technique for introducing the ROS sensors uniformly (Fig. 2), causing less damage to photosynthetic processes than vacuum infiltration (Table 2).

Production of $^1O_2$ by exposing leaves to excess PAR

Confocal LSM studies of spinach leaves infiltrated with either DanePy or using the pinhole method showed that the ROS sensors penetrated into the cells and were localised — at least partly — in the chloroplasts (Fig. 3). This confirmed the localisation of DanePy in *Arabidopsis* leaves (Hideg et al. 2001) and was a new finding about HO-1889NH. Fluorescence from both DanePy and HO-1889NH was quenched by exposing the leaves to excess PAR (Fig. 4, 5). Quenching of DanePy fluorescence has been reported in *Arabidopsis* leaves by excess PAR (Hideg et al. 2001). In the present study, quantitative analysis of DanePy fluorescence showed that the excess PAR-induced decrease mainly occurred in chloroplasts (Fig. 4). We found no excess PAR effect on the confocal LSM fluorescence images of dansyl-chloride either in *Arabidopsis* (Hideg et al. 2001) or in spinach leaves (data not shown). Dansyl-chloride contains the fluorescent moiety of the sensors but does not contain the spin trap.

Because HO-1889NH is specific to both $^1O_2$ and $O_2^{-\bullet}$, decrease in its fluorescence in leaves exposed to excess PAR (Fig. 5, 7) may be explained as a result of $^1O_2$ production, which was also detected with DanePy (Fig. 4, 6). On the other hand, it may also indicate the presence of $O_2^{-\bullet}$ besides $^1O_2$. In isolated membrane preparations, superoxide radicals have been implied to participate in photoinhibition as products of electron transport to oxygen both in functioning (Miyao 1994) and in donor-side impaired PSII (Chen et al. 1995), and recently in PSI (Tjus et al. 2001), although their production was not confirmed with spin trapping EPR spectroscopy (Hideg et al. 1995). In our experiments, HO-1889NH was less sensitive to $^1O_2$ than DanePy (Table 1), and its fluorescence was quenched to a smaller extent than in that of DanePy in spinach leaves exposed to excess PAR (Fig. 6, 7). As ROS sensors reached inside the leaves and had similar localisation (Fig. 3), our data suggest that the main product of photoinhibition in leaves is $^1O_2$ and the contribution of $O_2^{-\bullet}$ is minor.

The effect of ultraviolet radiation

Our earlier results with tobacco leaf disks which were vacuum infiltrated with DanePy suggested that $^1O_2$ production was not a characteristic product of UV-B stress (Hideg et al. 2000b). In the present study, we used whole spinach leaves and studied stress-induced changes in the fluorescence of ROS sensors which were infiltrated into the leaves through pinholes. A broad band (280–360 nm) UV source was used including both UV-B and UV-A. In experiments with DanePy infiltrated leaves, fluorescence emission from the ROS sensor was not markedly influenced by the UV treatment: 60 min irradiation resulting in more than 90% loss of photosynthetic activity caused only 8% loss of DanePy fluorescence, which was less than the uncertainty of the measurement (15%) (Fig. 6). In this way, our data confirmed that $^1O_2$ was not produced by a combination of UV-A and UV-B radiation.

On the other hand, the same radiation treatment caused a large, progressive quenching of HO-1889NH fluorescence (Fig. 7). Because we found no significant ROS production under identical conditions with the singlet oxygen trap DanePy (Fig. 6), stress-induced changes in HO-1889NH fluorescence should be explained as reaction of the ROS trap with $O_2^{-\bullet}$.

Indirect evidence for $O_2^{-\bullet}$ production in *Arabidopsis* plants was reported during long treatment (6–30 h) by UV-B but not by UV-A, on the basis of retarded induction of stress related genes in SOD sprayed leaves (A.-H.-Mackerness et al. 1998, A.-H.-Mackerness et al. 2001). On the other hand, activation of the plants' own superoxide dismutase enzymes by UV-B treatment has also been reported in higher plants (Rao and Ormrod 1995) as well as in *Chlorella* (Malanga and Puntarulo 1995). As in our experiments treatment times were shorter (maximum 1 h) and UV irradiation was stronger than in the above reports, the observed $O_2^{-\bullet}$ (Fig. 7) is more likely associated with damage to the photosynthetic apparatus, although it cannot be excluded that some of these may also act as signals for repair. Our earlier spin trapping EPR studies showed that the first ROS generated in UV-B exposed isolated thylakoid membranes were hydroxyl radicals (Hideg and Vass 1996) and $O_2^{-\bullet}$ was not observed in these samples with HO-1889NH, the fluorescent $O_2^{-\bullet}$ sensor either (Barta and Hideg, unpublished results). This suggests, that although in our UV irradiation experiment $O_2^{-\bullet}$ production was correlated with loss of photosynthetic activity of the leaf, the source of $O_2^{-\bullet}$ production is either selectively activated by longer wavelength UV or is present in leaves but missing from photosynthetic membrane preparations.

Materials and Methods

Plant material and stress conditions

Garden pea (*Pisum sativum*) leaves were grown, under 50 μmol m^{-2} s^{-1} PAR (16 h light/8 h dark), at 25°C for 5 weeks from sowing. Tobacco (*Nicotiana tabaccum* L.) plants were grown in the greenhouse under natural light conditions, at 22–25°C for 4–5 weeks from sowing. Mature spinach leaves were purchased at the local market in bundles with roots in moistened sponge and used the same day. All stress experiments were performed with detached spinach leaves while keeping petioles wet with watered tissue paper.

Adaxial leaf sides were exposed to either PAR from a KL-1500 lamp at 1,800 μmol m^{-2} s^{-1} (DMP, Switzerland) or to UV irradiation from a Supercure 203S source (San-Ei Electric Co., Japan) through a UG11+DUG11 (280–360 nm) band pass filter at 10 W m^{-2}. PAR and UV irradiances were determined by a PAR quantum sensor and an SD104βcos sensor, respectively, using a LI-COR LI-250 radiometer (LI-COR, U.S.A.). The UV sensor's peak sensitivity was at 313 nm, with half sensitivity at 298 and 327 nm, and less than 1% sensitivity below 280 nm and above 360 nm.

Parameters for the maximum quantum yield of PSII, F_v/F_m, and the electron transport rate, $\Delta F/F_m'$ (Genty et al. 1989), were measured with either a PAM-100 or a mini-PAM chlorophyll fluorometer (Walz,

Effeltrich, Germany). F_v/F_m was determined in leaves dark adapted for 15 min, and $\Delta F/F_m'$ was measured under 120 μmol m^{-2} s^{-1} actinic light. Spinach leaves, for example, show typical F_v/F_m and $\Delta F/F_m'$ values 0.782±0.076 and 0.488±0.038, respectively. The effect of photoinhibition by excess PAR and UV radiation was assessed by the decrease in $\Delta F/F_m'$ and the extent of damage was expressed as percentage loss as compared to untreated leaves.

The CO_2-fixation rate was determined using the portable photosynthetic system HCM-1000 (Walz, Effeltrich, Germany) under the following conditions: 370 ppm CO_2 in air, 25°C and 200 μmol m^{-2} s^{-1} PAR. Untreated leaves gave a fixation rate of 6.0 μmol CO_2 m^{-2} s^{-1}.

ROS sensors

For ROS detection, leaves or leaf segments were infiltrated with either 1 mM DanePy (Kálai et al. 1998) or 1 mM HO-1889NH (Kálai et al. 2002), in water solution, containing less than 5% ethanol by one of the following three methods. Vacuum infiltration was done inside a plastic syringe, within 15–20 s, as described earlier (Hideg et al. 1998). Uptake of the sensor by transpiration stream was carried out by immersing the petiole in the sensor solution overnight in the dark. The third was a method used for introducing pathogens to leaves as initiated by Prof. T. Shiraishi (Okayama University, Japan): the sensor solution (approx 10–20 μl) was forced into the leaf tissue using a plastic syringe without the needle into the middle layer, through a pinhole of the tissue made at the adaxial side with a sharp pin.

Fluorescence spectroscopy

The fluorescence emission spectrum of ROS sensors was recorded at room temperature, with a Quanta Master QM-1 (Photon Technology Int. Inc., U.S.A.) spectrofluorometer using 330 nm excitation. For ROS selectivity experiments, fluorescence was measured in a quartz cuvette during continuous stirring in 0.2 mM solutions of one of the ROS sensors in Na-phosphate buffer (50 mM, pH 7.2). Relative changes in the sensor's fluorescence were induced by trapping various chemically induced ROS. Singlet oxygen ($^1O_2$) was generated from illuminating 30 μg ml^{-1} Triton-extracted chlorophyll by 500 μmol m^{-2} s^{-1} PAR. Hydroxyl radicals ($^{\bullet}OH$) were produced from 0.2 mM H_2O_2 — which was also applied independently — and 0.2 mM Fe(II) from ammonium ferrous sulfate. Superoxide anion radicals ($O_2^{-\bullet}$) were generated from illuminating 0.06 mM riboflavin by 500 μmol m^{-2} s^{-1} PAR. Five min after the ROS generating reaction under the above conditions fluorescence quenching was determined as described earlier (Kálai et al. 1998).

In leaf experiments, 2 cm long cuttings of leaves before and after ROS sensor infiltration were positioned on a metal sample holder, at a 45° angle to both excitation and emission axis with their adaxial side uppermost. In order to avoid the effect of any stray light, 0° and 90° polarisers were used in front of the excitation and emission monochromators, respectively. Excitation and emission slits were both 4 nm. In order to improve signal : noise ratio, five spectra were collected and averaged from the same sample to form one spectrum. Before determining fluorescence maxima, these raw data were smoothed by calculating a weighted average of neighbouring points. ROS detection was based on the decrease of sensor fluorescence, as described earlier (Hideg et al. 1998).

Fluorescence imaging

In all imaging experiments, fluorescence images were recorded from detached leaves positioned flat, with adaxial sides uppermost on black paper. Experiments comparing the localisation of ROS in leaves after various infiltration methods were carried out using an Epi-LightUV FA500 monochrome CCD camera imaging system (AISIN Taitec, Kosmos Kenkyo Inc., Japan), equipped with 310 nm (10 nm bandwidth) excitation. The manufacturer's emission filter was replaced with a BG18 (410–640 nm) band pass filter and fluorescence images were collected using the instrument's image capture facility.

For quantitative analysis, ROS sensor infiltrated spinach leaves were studied with a Leica MZ FL III Microscope (Leica Microsystems, Tokyo, Japan) using 1.5 magnification. Instead of using the microscope's own lamp, fluorescence was excited with 280–360 nm UV radiation from the Supercure 203S source (San-Ei Electric Co., Japan) through a UG11+DUG11 band pass filter combination (295–375 nm) from above. Fluorescence emission was detected through a BG18 (410–640 nm) band pass filter by a digital image analysing system (Pixera Viewfinder 2.5, Pixera Corp., U.S.A.). All images were collected using identical focus and pinhole settings. For evaluating ROS-induced fluorescence quenching, individual images were converted to greyscale and evaluated using the free UTHSCSA ImageTool program, developed at the University of Texas Health Science Center (San Antonio, Texas, U.S.A.) and available from the Internet by anonymous FTP from ftp://maxrad6.uthscsa.edu.

Confocal LSM

Leaf cuttings (6×6 mm) including the area infiltrated with the ROS sensor were sandwiched between two layers of UV-transparent microscope cover glass (MicroStandard Cover Glass, Matsumi Glass, Japan) and measured using a confocal laser scanning system (LSM 510, Karl Zeiss, Germany) in combination with an inverted microscope (Axiovert 100 M, Karl Zeiss, Germany). Adaxial sides of the leaf segments faced the 351 nm Ar laser excitation (80 mW, ENTCII-653, Coherent Enterprise, Santa, California, U.S.A.). Fluorescence emission was observed through filters: 515–550 nm for green and above 650 nm for red fluorescence from a 115×115 μm area. Images were scanned at 0.8 s per frame, averaging four images. LSM images have false colour coding. For example, all fluorescence detected in the 515–550 nm spectral region is shown in the same monochrome green, regardless of its actual wavelength.

Quantitative analysis of the LSM images was carried out according to three strategies: (1) in order to study the localisation of the ROS sensor inside the leaf, we matched the intensity distributions of green (ROS sensor) and red (chlorophyll) fluorescence along the same line on the same image in leaves without stress. In order to characterise stress-induced changes of green (ROS) fluorescence we compared either (2) intensity distributions along a chosen line or (3) histograms using a series of images acquired after exposure to PI or UV radiation for various times. These data were generated using the profile and histogram generating feature of the LSM software.

Acknowledgments

Research at Szeged was supported by the Hungarian National Research Foundation (OTKA T-030262). Collaboration between the Hungarian and Japanese laboratories was supported by the Hungarian Science and Technology Foundation (TéT JAP 8/98) and by a Grant-In-Aid for Scientific Research from the Ministry of Education, Science and Culture, Japan. We thank Prof. Y. Yamaguchi (Department of Biotechnology, Fukuyama University) for his help with setting up the fluorescence imaging systems and Mr. T. Owaki for doing the CO_2 assimilation rate measurements. Synthesis and development of the ROS sensors was partly funded by the Hungarian National Research Foundation (OTKA T-034307).

References

A.-H.-Mackerness, S., John, C.F., Jordan, B. and Thomas, B. (2001) Early signaling components in ultraviolet-B responses: distinct roles for different reac-

tive oxygen species and nitric oxide. *FEBS Lett.* 489: 237–242.

A.-H.-Mackerness, S., Surplus, S.L., Jordan, B.R. and Thomas, B. (1998) Effects of supplementary ultraviolet-B radiation on photosynthetic transcripts at different stages of leaf development and light levels in pea (*Pisum sativum* L.): role of active oxygen species and antioxidant enzymes. *Photochem. Photobiol.* 68: 88–96.

Andersson, B. and Barber, J. (1996) Mechanisms of photodamage and protein degradation during photoinhibition of photosystem II. *In* Photosynthesis and the Environment. Edited by Baker, N.R. pp. 101–121. Kluwer Academic Publishers, Dordrecht.

Aro, E.-M., Virgin, I. and Andersson, B. (1993) Photoinhibition of photosystem II: inactivation, protein damage and turnover. *Biochim. Biophys. Acta* 1143: 113–134.

Asada, K. (1994) Production and action of active oxygen species in photosynthetic tissues. *In* Causes of Photooxidative Stress and Amelioration of Defence Systems in Plants. Edited by Foyer, Ch. and Mullineaux, P.M. pp. 77–104. CRC Press, Boca Raton.

Asada, K. (1999) The water-water cycle in chloroplasts: Scavenging of active oxygens and dissipation of excess photons. *Annu. Rev. Plant Physiol. Plant Mol. Biol.* 50: 601–639.

Barber, J. and Andersson, B. (1992) Too much of a good thing: light can be bad for photosynthesis. *Trends Biochem. Sci.* 17: 61–66.

Bornman, J.F. (1989) New trends in photobiology. Target sites of UV-B radiation in photosynthesis of higher plants. *J. Photochem. Photobiol.* 4: 145–158.

Chapelle, E.W., Wood, F.M., McMurtrey, J.E. and Newcourt, W.W. (1984) Laser-induced fluorescence of green plants. 1: A technique for remote detection of plant stress and species differentiation. *Appl. Optics* 23: 134–138.

Chen, G.-X., Blubaugh, D.J., Homann, P.H., Golbeck, J.H. and Cheniae, G.M. (1995) Superoxide contributes to the rapid inactivation of specific secondary donors of the photosystem II reaction center during photodamage of manganese-depleted photosystem II membranes. *Biochemistry* 34: 2317–2332.

Friso, G., Spetea, C., Giacometti, G.M., Vass, I. and Barbato, R. (1994) Degradation of photosystem II reaction centre D1 protein induced by UV-B radiation in isolated thylakoids. Identification and characterization of C- and N-terminal breakdown products. *Biochim. Biophys. Acta* 1184: 78–84.

Genty, B., Briantais, J.M. and Baker N.R. (1989) The relationship between the quantum yield of photosynthetic electron-transport and quenching of chlorophyll fluorescence, *Biochim. Biophys. Acta* 990: 87–92.

Green, S.A., Simpson, D.J., Zhou, G., Ho, P.S. and Blough, N.V. (1990) Intramolecular quenching of excited singlet states by stable nitroxyl radicals. *J. Amer. Chem. Soc.* 112: 7337–7346.

Greenberg, B.M., Gaba, V., Canaani, O., Malkin, S. and Edelman, M. (1989) Separate photosensitizers mediate degradation of the 32kDa reaction centre II protein in visible and UV-spectral regions. *Proc. Natl. Acad. Sci. USA* 86: 6617–6620.

Halliwell, B. and Gutteridge, J.M.C. (1999) *Free Radicals in Biology and Medicine*. Oxford University Press, Oxford.

Hankovszky, H.O., Kálai, T., Hideg, É., Jekő, J. and Hideg, K. (2001) Synthesis and study of double (EPR active and fluorescent) chemosensors in the presence of Fe^{3+} ion. *Synth. Commun.* 31: 975–986.

Hideg, É., Kálai, T., Hideg, K. and Vass, I. (1998) Photoinhibition of photosynthesis in vivo results in singlet oxygen production. Detection via nitroxide-induced fluorescence quenching in broad bean leaves. *Biochemistry* 37: 11405–11411.

Hideg, É., Kálai, T., Hideg, K. and Vass, I. (2000b) Do oxidative stress conditions impairing photosynthesis in the light manifest as photoinhibition? *Philos. Trans. R. Soc. London B* 355: 1511–1516.

Hideg, É., Ogawa, K., Kálai, T. and Hideg, K. (2001) Singlet oxygen imaging in *Arabidopsis thaliana* leaves under photoinhibition by excess photosynthetically active radiation. *Physiol. Plant.* 112: 10–13.

Hideg, É., Spetea, C. and Vass, I. (1994a) Singlet oxygen and free radical production during acceptor- and donor-side-induced photoinhibition. Studies with spin trapping EPR spectroscopy. *Biochim. Biophys. Acta* 1186: 143–152.

Hideg, É., Spetea, C. and Vass, I. (1994b) Singlet oxygen production in thylakoid membranes during photoinhibition as detected by EPR spectroscopy. *Photosynth. Res.* 39: 191–199.

Hideg, É., Spetea, C. and Vass, I. (1995) Superoxide radicals are not the main promoters of acceptor side induced photoinhibitory damage in spinach thylakoids. *Photosynth. Res.* 46: 399–407.

Hideg, É. and Vass, I. (1996) UV-B induced free radical production in plant leaves and isolated thylakoid membranes. *Plant Sci.* 115: 251–260.

Hideg, É., Vass, I., Kálai, T. and Hideg, K. (2000a) Singlet oxygen detection with sterically hindered amine derivatives in plants under light stress. *Methods Enzymol.* 319: 77–85.

Hirayama, S., Ueda, R. and Sugata, K. (1995) Detection of hydroxyl radical in intact cells of *Chlorella vulgaris*. *Free Radic. Res.* 23: 51–59.

Kálai, T., Hankovszky, O.H., Hideg, É., Jekő, J. and Hideg, K. (2002) Synthesis and structure optimalization of double (fluorescent and spin) sensor molecules. *ARKIVOC* 2002 (iii): 112–120.

Kálai, T., Hideg, É., Vass, I. and Hideg, K. (1998) Double (fluorescent and spin) sensors for detection of reactive oxygen species in the thylakoid membrane. *Free Rad. Biol. Med.* 24: 649–652.

Kulandaivelu, G. and Noorudeen, A.M. (1983) Comparative study of the action of ultraviolet-C and ultraviolet-B radiation on photosynthetic electron transport. *Physiol. Plant.* 58: 389–394.

Malanga, G. and Puntarulo, S. (1995) Oxidative stress and antioxidant content in *Chlorella vulgaris* after exposure to ultraviolet-B radiation. *Physiol. Plant.* 94: 672–679.

Miyao, M. (1994) Involvement of active oxygen species in degradation of the D1 protein under strong illumination in isolated subcomplexes of photosystem II. *Biochemistry* 33: 9722–9730.

Powles, S.B. (1984) Photoinhibition of photosynthesis induced by visible light. *Annu. Rev. Plant Physiol.* 35: 15–44.

Rao, M.V. and Ormrod, D.P. (1995) Impact of UVB and O_3 on the oxygen free radical scavenging system in *Arabidopsis thaliana* genotypes differing in flavonoid biosynthesis. *Photochem. Photobiol.* 62: 719–726.

Renger, G., Volker, M., Eckert, H.J., Fromme, R., Hohm-Veit, S. and Graber, P. (1989) On the mechanism of photosystem II deterioration by UV-B irradiation. *Photochem. Photobiol.* 49: 97–105.

Teramura, A.H. and Sullivan, J.H. (1994) Effects of UV-B radiation on photosynthesis and growth of terrestrial plants. *Photosynth. Res.* 39: 463–473.

Tjus, S.E., Scheller, H.V., Andersson, B. and Møller, B.L. (2001) Active oxygen production during selective excitation of photosystem I is damaging not only to photosystem I, but also to photosystem II. *Plant Physiol.* 125: 2007–2015.

Vass, I. (1997) Adverse effects of UV-B light on the structure and function of the photosynthetic apparatus. *In* Handbook of Photosynthesis. Edited by Pessarakli, M. pp. 931–949. Marcel Dekker, New York.

Vass, I., Sass, L., Spetea, C., Bakou, A., Ghanotakis, D. and Petrouleas, V. (1996) UV-B induced inhibition of photosystem II electron transport studied by EPR and chlorophyll fluorescence. Impairment of donor and acceptor side components. *Biochemistry* 35: 8964–8973.

Yruela, I., Pueyo, J.J., Alonso, P.J. and Picorel, R. (1996) Photoinhibition of photosystem II in plants: effect of copper inhibition. *J. Biol. Chem.* 271: 27408–27415.

(Received April 15, 2002; Accepted July 21, 2002)